Automatika

Journal for Control, Measurement, Electronics, Computing and Communications

ISSN: (Print) (Online) Journal homepage: www.tandfonline.com/journals/taut20

FAT-based adaptive and velocity feedback control of cooperative manipulators handling a flexible object

Abdul Rahman Samewoi, Norsinnira Zainul Azlan & Md. Raisuddin Khan

To cite this article: Abdul Rahman Samewoi, Norsinnira Zainul Azlan & Md. Raisuddin Khan (2023) FAT-based adaptive and velocity feedback control of cooperative manipulators handling a flexible object, Automatika, 64:4, 1010-1025, DOI: 10.1080/00051144.2023.2236857

To link to this article: https://doi.org/10.1080/00051144.2023.2236857

Published online: 02 Aug 2023.

AUTOMATIKA
2023, VOL. 64, NO. 4, 1010–1025
https://doi.org/10.1080/00051144.2023.2236857

FAT-based adaptive and velocity feedback control of cooperative manipulators handling a flexible object

Abdul Rahman Samewoi, Norsinnira Zainul Azlan and Md. Raisuddin Khan

Department of Mechatronics Engineering, International Islamic University Malaysia, Kuala Lumpur, Malaysia

ABSTRACT

The previous regressor-based control method to control two cooperative manipulators in handling a deformable object leads to complex calculations and complicated programming in experimental hardware tests. There is an existing lack of studies about the development of the controller based on a partial differential equation (PDE)-based model and considering the model's uncertainties. Previous studies have shown fewer experimental validations regarding two cooperative manipulators that handle deformable objects under uncertain model parameters. This study proposes a composite controller comprising a function approximation technique (FAT)-based adaptive control (FATAC) for a slow subsystem and a velocity feedback control (VFC) for a fast subsystem. The proposed FATAC is used for trajectory tracking, and VFC is used to suppress the vibration of the deformable object. Lyapunov stability analysis has been carried out to design controllers that stabilize a non-linear system of two cooperative manipulators handling the flexible object. Simulation and hardware experimental tests have been carried out to validate the performance of proposed controllers. The results verified that the proposed composite controller comprising the FATAC has successfully driven the cooperative manipulators to handle the deformable object so that it follows the desired trajectories. The VFC has successfully suppressed the transverse vibration of the deformable object.

ARTICLE HISTORY
Received 14 February 2021
Accepted 11 July 2023

KEYWORDS
Composite control; slow-fast subsystems; flexible beam; function approximation technique

1. Introduction

Many tasks can be effectively performed in various industrial applications using at least two manipulators. Similar to humans, using two arms to perform a single task has more advantages than using a single arm. The main applications of such manipulators can be realized in transporting massive objects, assembling automotive parts, and handling deformable objects. Deformable objects may be classified as one-dimensional such as a flexible beam, two-dimensional, such as a flexible sheet, or three-dimensional, such as a flexible body [1]. An extensive literature review has been completed with regards to the dynamic model of deformable objects and found that several methods have been used in previous studies, such as the simple model system [2,3], the finite element method (FEM) [4,5], the assumed mode method (AMM) [6–8], and the partial differential equation (PDE) system [9–11]. It is also found that the flexible beam is a popular deformable object handled by cooperative manipulators. In grasping and moving the flexible beam by two cooperative manipulators, several studies have reported trajectory tracking of the mass center of the flexible beam while suppressing its vibration [5,7,9,12,13].

Two strategies were used to control two cooperative manipulators while handling a deformable object. The first method is a model-free method [14–16] with a disadvantage: it excludes the mathematical modeling that describes the equations of motion. The equations of motion are essential in the design of robots, simulation and animation of robot motion, and the design of control algorithms [17]. The second control method is a modeled-based method widely used to control two cooperative manipulators in handling a flexible object and suppressing the vibration. Several types of controllers were proposed, such as hybrid impedance controller [18] and hybrid position and force controller [19,20], which were used to stabilize the system, suppress the vibration, and control internal forces between two manipulators and the beam. A computational scheme was developed to determine the optimal trajectory, and vibration was also suppressed [6]. An internal force-based impedance controller was proposed to control the internal force while deforming the object to reach the desired shape [2]. Sliding mode control was proposed to provide robustness against model imperfection and uncertainty and suppress the vibration [7]. Two-time scale controllers were presented in a PD control scheme for the rigid motion to track the desired trajectory and a pole placement technique for the flexible motion to suppress the vibration [8]. Meanwhile, another study proposed an adaptive sliding mode

CONTACT Norsinnira Zainul Azlan sinnira@iium.edu.my Department of Mechatronics Engineering, International Islamic University Malaysia, Kuala Lumpur 53100, Malaysia

control for the slow subsystem and suggested a robust optimal control for the fast subsystem [5].

As previously mentioned, most control designs for two cooperative manipulators handling a deformable object are based on the FEM or the AMM mathematical modeling. Although the FEM and the AMM yield detailed and precise mathematical models, the methods have truncated the model of the flexible object with an infinite degree of freedom to a finite-dimensional model, leading to several drawbacks in control design [21]. Several studies have presented different approaches without using the FEM or the AMM. A simple boundary control law to address the synchronization issue of the system consists of two manipulators and a flexible beam [10]. However, only simulation results were demonstrated in their work. An adaptive barrier control was developed to suppress the beam's vibration without violating the constraint [22]. However, the implementation of the proposed control was not discussed. Another research suggested a model-based method of calculating the cooperative manipulators' inverse and direct dynamic model in handling flexible objects [4]. Nonetheless, the study did not have the control scheme designs, and no experimental validation was presented. In addition, a method for learning force-based manipulation skills from demonstrations was also presented using non-rigid registration to compute a warping function that transforms both the end-effector poses and forces each demonstration into the current scene [23].

Since the control design, based on the FEM and the AMM mathematical modeling, has truncated the model of the flexible object with an infinite degree of freedom to a finite-dimensional model, it has several drawbacks to the control design [21], which are (i) it requires as many sensors as the locations of the measurement of the vibration and the difficulty in the implementation, (ii) it leads to the presence of the control and the observation spillover due to ignored high-frequency dynamics, (iii) it is often not clear how many modes must be considered to approximate the PDE-based model into the ordinary differential equation (ODE) model, (iv) it destabilizes the system due to the negligence of higher-order modes, and (v) it requires a higher-order controller. The drawbacks can be improved by deriving dynamics equations of cooperative manipulators handling a deformable object and presenting it in the PDE system [9,21]. The PDE-based model provides several advantages, such as avoiding using many sensors to measure the vibration, considering higher-order modes leading to the system destabilization, and preventing the control and observation spillover.

In controlling the manipulators-beam system without using any approximation methods, a composite controller is designed by combining the robust sliding mode control for the slow subsystem and the velocity feedback controller for the fast subsystem. Simulation results demonstrated that the proposed control approach could achieve satisfactory tracking performance while suppressing the vibration of the beam. However, there were complex regressor calculations in designing the control law in [9], which has been improved by formulating a robust adaptive control law [24]. The PDE-based model in [9] has been further studied to analyze kinematics and validate the trajectory [25]. Using a similar model, the computed torque control (CTC) scheme has been implemented on the slow subsystem for trajectory tracking, and a velocity feedback control (VFC) is designed for the fast subsystem to suppress the vibration [26]. However, the CTC scheme requires the exact model to be known, which is impossible to achieve in the actual hardware implementation.

From the literature survey, a lack of research was conducted on developing a controller based on the PDE-based model by considering the model uncertainties, although the PDE-based system offers many advantages. Some studies have used the regressor-based method to design the control, leading to complex calculations and complicated programming in the experimental hardware test. There is also a lack of experimental validations that have been done in previous works regarding two cooperative manipulators in handling deformable objects. Therefore, the novelty of this research is the implementation of a composite controller comprising a function approximation technique (FAT)-based adaptive control (FATAC) for a slow subsystem and the VFC for a fast subsystem for two cooperative manipulators handling the flexible beam that is modeled-based on the PDE.

The contributions of the proposed FATAC in this paper include (1) how it can overcome model uncertainties and is easy to be programmed for hardware implementation since it does not involve tedious calculations, such as in the CTC scheme. In an actual application, the precise dynamics of two cooperative manipulators in handling a flexible beam are unknown. Thus, the traditional computed torqued controller cannot be used [27]. Some complex dynamics, such as joint flexibility, actuators, and time-varying payloads, are ignored because the dynamics modeling is highly complex, leading to the difficulty in designing a controller. The estimation of system parameters in this complex model becomes more challenging. Thus, some system dynamics are regarded as uncertainties to simplify the dynamics modeling. Robust controls and adaptive controls are proposed to deal with these uncertainties. However, they need knowledge of the variation bounds for the uncertainties. They also need to use the tedious regressor matrix to derive, which is highly computational and challenging to be programmed. There are two

types of uncertainties which are time-constant uncertainties and time-varying uncertainties. When the system contains time-varying uncertainties whose variation bounds are not given, robust control and adaptive design are not feasible [27]. This suggests the need for regressor-free adaptive designs, known as the FATAC, representing general uncertainties in the cooperative robots' model as finite combinations of weighted basis functions with unknown constant coefficients [27] (2) can provide an alternative method of designing a controller without using the FEM and AMM, as they have several drawbacks, as mentioned earlier.

Alternatively, the FATAC has been designed based on the PDE-based model, (3) hardware experimental set-up and test for controlling the cooperative manipulators in handling the flexible beam, which is not discussed extensively in previous studies. Thus, to further explore the idea, Section 2 of this paper provides the kinematics and dynamics of the cooperative manipulators and the flexible beam, while Section 3 includes composite control, which consists of the FATAC for the slow subsystem and the VFC for the fast subsystem. The stability analysis is also presented using a suitable Lyapunov candidate to derive the control law. The simulation results are presented in Section 4 to prove the feasibility of the proposed controllers, and the experimental results are presented in Section 5 to verify the proposed controller experimentally. Section 6 will conclude the paper.

2. Kinematics the system

The system consists of two identical planar and three degree-of-freedom (DOF) cooperative manipulators handling a flexible beam, as shown in Figure 1. Each manipulator has three rigid links with three revolute joints. For two cooperative manipulators, the trajectory validation and kinematics analysis, which includes the forward and inverse kinematics equations, are stated in [25]. For a flexible beam, its length, L and mass, $m = \rho L$ are considered in deriving the kinematics, where ρ is the density of the flexible beam. The coordinate frame, X_rY_r is fixed frame and xy-frame is a moving coordinate frame which is attached to the midpoint of the beam, X_{mp} [9] as stated by

$$X_{mp} = \begin{Bmatrix} x_o & y_o & \theta \end{Bmatrix}^T \tag{1}$$

where x, y and θ represent X-position, Y-position, and the orientation, respectively. F_{1x}, , F_{2x}, and F are forces applied by the manipulators at the two ends of the beam, as shown in Figure 2. The transverse displacement, $\eta(x,t)$ is a flexible parameter measured with respect to the xy-frame which varies with a time, t and a spatial coordinate, x ranging from $-L/2$ to $+L/2$ [9]. By neglecting the deformation in a longitudinal direction, all the kinematic relations are derived with respect to X_rY_r-frame as in [9]. This means that the equation will hold for small bending angles.

3. Dynamics of the system

3.1. Cooperative manipulators dynamics

The general dynamics equation for 3-DOF and planar manipulator [28] can be expressed as

$$\begin{aligned} M_i(q_i)\ddot{q}_i + C_i(q_i,\dot{q}_i)\dot{q}_i + G_i(q_i) \\ = \tau_i + J_i^T f_i \end{aligned} \tag{2}$$

where

$$M_i(q_i) = \begin{bmatrix} m_{i11} & m_{i12} & m_{i13} \\ m_{i21} & m_{i22} & m_{i23} \\ m_{i31} & m_{i32} & m_{i33} \end{bmatrix},$$

$$C_i(q_i,\dot{q}_i) = \begin{bmatrix} c_{i11} & c_{i12} & c_{i13} \\ c_{i21} & c_{i22} & c_{i23} \\ c_{i31} & c_{i32} & c_{i33} \end{bmatrix},$$

$$G_i(q_i) = \begin{Bmatrix} g_{i1} \\ g_{i2} \\ g_{i3} \end{Bmatrix}, J_i(q_i) = \begin{bmatrix} J_{i11} & J_{i12} & J_{i13} \\ J_{i21} & J_{i22} & J_{i23} \\ 1 & 1 & 1 \end{bmatrix},$$

$$\tau_i = \begin{Bmatrix} \tau_{i1} \\ \tau_{i2} \\ \tau_{i3} \end{Bmatrix}, f_i = \begin{Bmatrix} f_{i1} \\ f_{i2} \\ f_{i3} \end{Bmatrix}, \dot{q}_i = \begin{Bmatrix} \dot{q}_{i1} \\ \dot{q}_{i2} \\ \dot{q}_{i3} \end{Bmatrix},$$

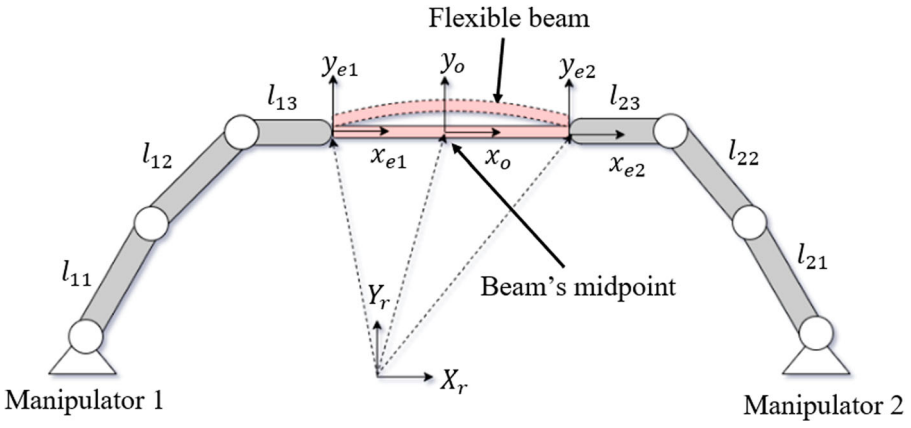

Figure 1. Two planar and cooperative manipulators handling a flexible beam.

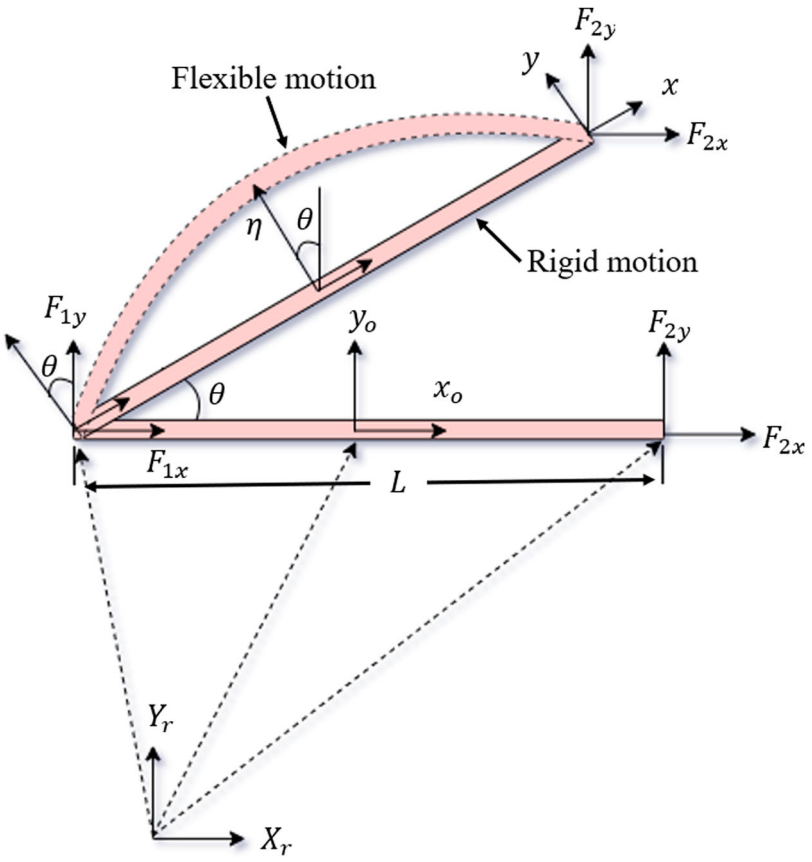

Figure 2. Schematic diagram of the beam.

$$\ddot{q}_i = \begin{Bmatrix} \ddot{q}_{i1} \\ \ddot{q}_{i2} \\ \ddot{q}_{i3} \end{Bmatrix} \tag{3}$$

q, $\dot{q}_i$, and $\ddot{q}_i$ are 3×1 vectors of generalized joint displacements, velocities, and accelerations, respectively. $M_i(q_i)$ is a 3×3 symmetric positive definite inertia matrix, $C_i(q_i, \dot{q}_i)$ is a 3×3 coriolis and centrifugal matrix, $G_i(q_i)$ is a 3×1 vector of gravitational components, $J_i(q_i)$ is a 3×3 Jacobian matrix of the manipulators, τ_i is a 3×1 vector of input torque applied at each joint of the manipulators, and f_i is a 3×1 vector of the interaction force between the manipulators and the flexible beam. Therefore, the dynamics equations for two 3-DOF and planar cooperative manipulators can be written in a joint space as

$$M_m \ddot{q} + C_m \dot{q} + G_m = \tau + J^T f \tag{4}$$

where

$$M_m = \begin{bmatrix} M_1 & 0 \\ 0 & M_2 \end{bmatrix}, C_m = \begin{bmatrix} C_1 & 0 \\ 0 & C_2 \end{bmatrix},$$
$$G_m = \begin{Bmatrix} G_1 \\ G_2 \end{Bmatrix}, J = \begin{bmatrix} J_1 & 0 \\ 0 & J_2 \end{bmatrix},$$
$$\tau = \begin{Bmatrix} \tau_1 \\ \tau_2 \end{Bmatrix}, f = \begin{Bmatrix} f_1 \\ f_2 \end{Bmatrix}, \dot{q} = \begin{Bmatrix} \dot{q}_1 \\ \dot{q}_2 \end{Bmatrix},$$
$$\ddot{q} = \begin{Bmatrix} \ddot{q}_1 \\ \ddot{q}_2 \end{Bmatrix}, \tag{5}$$

Note that M_i, C_i, G_i, J_i, τ_i, f_i, $\dot{q}_i$, and $\ddot{q}_i$ are from equation (3) that represents i-th manipulator. All matrix or vector elements of dynamics of two cooperative manipulators can be found in [28] and [26].

3.2. Flexible beam dynamics

The dynamics of the beam are derived by using the extended Hamiltonian Principle [9] as

$$\int_{t_1}^{t_2} (\delta U - \delta T - \delta W)\, dt = 0 \tag{6}$$

where δU is the variation of the potential energy, U, δT is the variation of the kinetic energy, T, and δW is the work done due to external forces, W. Meanwhile, t_1 and t_2 are any two instances of the time with $t_2 > t_1 > 0$. Beam dynamics are presented in Cartesian coordinates comprising rigid dynamics and transverse vibration, which are flexible dynamics. Rigid dynamics of the beam can be represented in a compact form [9] as

$$M_{brf} \ddot{X}_{mp} + C_{brf} + \eta_{brf} + G_{brf} = F_{brf}(-f), \tag{7}$$

where

$$M_{brf} = \begin{bmatrix} m & 0 & M_{brf1} \\ 0 & m & M_{brf2} \\ M_{brf1} & M_{brf2} & M_{brf3} \end{bmatrix},$$

$$C_{brf} = \begin{Bmatrix} C_{brf1} \\ C_{brf2} \\ 0 \end{Bmatrix},$$

$$\eta_{brf} = \begin{Bmatrix} \eta_{brf1} \\ \eta_{brf2} \\ \eta_{brf3} \end{Bmatrix}, G_{brf} = \begin{Bmatrix} 0 \\ mg \\ 0 \end{Bmatrix},$$

$$\ddot{X}_{mp} = \begin{Bmatrix} \ddot{x}_0 \\ \ddot{y}_0 \\ \ddot{\theta} \end{Bmatrix},$$

$$F_{brf} = \begin{bmatrix} 1 & 0 & 0 & 1 & 0 & 0 \\ 0 & 1 & 0 & 0 & 1 & 0 \\ F_{brf1} & F_{brf2} & 0 & F_{brf3} & F_{brf4} & 0 \end{bmatrix},$$

$$f = \begin{Bmatrix} F_{1x} & F_{1y} & M_{O_1} & F_{2x} & F_{2y} & M_{O_2} \end{Bmatrix}^T \tag{8}$$

M_{brf} is a 3×3 inertia matrix of the beam with flexible and rigid parameters, C_{brf} is a 3×1 centrifugal vector of the beam with flexible and rigid parameters, η_{brf} is a 3×1 vibration vector of the beam with flexible parameters only, G_{brf} is a 3×1 gravitational vector of the beam with flexible and rigid parameters, F_{brf} is a 3×6 force transformation matrix with flexible and rigid parameters, f is a 6×1 forces/moments vector at the two ends of the manipulator, and $\ddot{X}_{mp}$ is a 3×1 acceleration vector of the beam's midpoint. The subscript "*brf*" is used to denote a matrix or a vector that consists of flexible and rigid parameters. All matrix or vector elements of rigid dynamics of the beam can be found in [28] and [26].

The transverse vibration of the beam [9] is presented as.

$$-\sin\theta\ddot{x}_o + \cos\theta\ddot{y}_o + x\ddot{\theta} + \ddot{\eta} - \eta\dot{\theta}^2 + \frac{EI}{\rho}\eta^{iv} = F_{ff}(f), \tag{9}$$

where

$$F_{ff} = \frac{1}{m}\begin{bmatrix} -\sin\theta & \cos\theta & 0 & -\sin\theta & \cos\theta & 0 \end{bmatrix} \tag{10}$$

t is the time, and x is a spatial coordinate. $m$is the mass of the flexible beam, ρ is the density of the beam, E is the moment of inertia of the beam, and I is Young's modulus of the beam. θ, $\dot{\theta}$, and $\ddot{\theta}$ are the orientation of the flexible beam's midpoint, the first derivative of θ with respect to t, and the second derivative of θ with respect to t, respectively. $\ddot{x}_o$ is the second derivative of the x-position of the beam's midpoint, x_o and $\ddot{y}_o$ is the second derivative of y-position of the beam's midpoint, y_o. F_{ff} and f are 1×6 force transformation matrix in the transverse vibration and 6×1 forces/moments vector at the two ends of the 3-DOF manipulator, respectively. η, $\ddot{\eta}$, and η^{iv} are the transverse displacement that varies with x and t, the second derivative of η with respect to t, and the fourth derivative of η with respect to x, respectively.

3.3. Combined dynamics and singular perturbation model

The dynamics of cooperative manipulators as equation (4) and the rigid dynamics of the beam as equation (7) are integrated to form combined rigid dynamics as.

$$M_{crf}\ddot{X}_{mp} + C_{crf}\dot{X}_{mp} + G_{crf} + \eta_{crf} = U_{crf} \tag{11}$$

where

$$\begin{aligned} M_{crf} &= {R_{rf}}^T J^{-T} M_m J^{-1} R_{rf} + M_{brf} \\ C_{crf} &= {R_{rf}}^T J^{-T}(M_m \dot{J}^{-1} R_{rf} \\ &\quad + M_m J^{-1}\dot{R}_{rf} + C_m J^{-1} R_{rf}) + C_{brf} \\ G_{crf} &= {R_{rf}}^T J^{-T} G_m + G_{brf} \\ \eta_{crf} &= \eta_{brf} \\ U_{crf} &= {R_{rf}}^T J^{-T}\tau \end{aligned} \tag{12}$$

The transverse vibration is still the same as equation (9), in which it involves the rigid and flexible parameters [9]. The system is highly non-linear that involves vibration and flexibility. The popular singular perturbation technique [29] is employed on combined rigid dynamics and transverse vibration. The method's purpose is to approximate solutions and reduce the order of the system model. From this method, two subsystems with different time scales are obtained: the slow and fast subsystems. Each subsystem has its function: the slow subsystem represents the rigid body motion without any flexible parameters. In contrast, the fast subsystem represents the transverse vibration of the flexible beam. The slow subsystem is produced when the flexible parameter in combined rigid dynamics and transverse vibration are decoupled and eliminated by introducing a new variable, $v(x,t)$ in the same order as the state variable [9] as

$$v(x,t) = \mu^2\eta(x,t), \tag{13}$$

where $\mu = 1/C$ is known as the perturbed parameter and C is a dimensionless parameter with a large value for different materials. The flexible parameter is eliminated by setting the perturbed parameter, μ as it approaches zero ($\mu \to 0$).

Therefore, the slow subsystem that represents the rigid body motion without involving any flexible parameters [9] is given as

$$M_{cr}\ddot{X}_{mp} + C_{cr}\dot{X}_{mp} + G_{cr} = U_{cr}, \tag{14}$$

where

$$\begin{aligned} M_{cr} &= R_r^T J^{-T} M_m J^{-1} R_r + M_{br} \\ C_{cr} &= R_r^T J^{-T}(M_m \dot{J}^{-1} R_r + M_m J^{-1}\dot{R}_r + C_m J^{-1} R_r) \\ G_{cr} &= R_r^T J^{-T} G_m + G_{br} \\ U_{cr} &= R_r^T J^{-T}\tau \end{aligned} \tag{15}$$

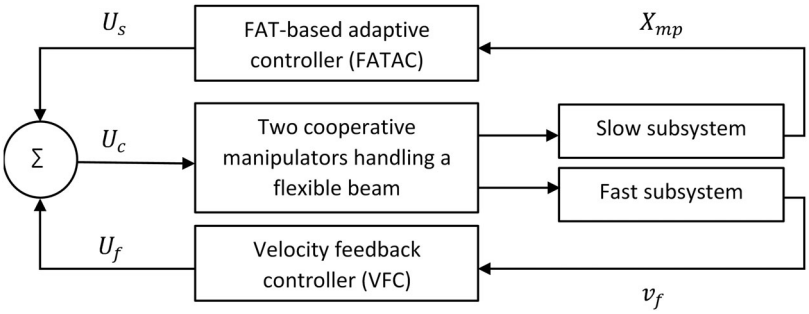

Figure 3. Block diagram of the proposed composite controller comprising the FATAC for the slow subsystem and the VFC for the fast subsystem.

and

$$M_{br} = \begin{bmatrix} m & 0 & 0 \\ 0 & m & 0 \\ 0 & 0 & \dfrac{mL^2}{12} \end{bmatrix}, G_{br} = \begin{Bmatrix} 0 \\ mg \\ 0 \end{Bmatrix},$$

$$R_r = \begin{bmatrix} 1 & 0 & \dfrac{L}{2}\sin\theta \\ 0 & 1 & -\dfrac{L}{2}\cos\theta \\ 0 & 0 & 1 \\ 1 & 0 & -\dfrac{L}{2}\sin\theta \\ 0 & 1 & \dfrac{L}{2}\cos\theta \\ 0 & 0 & 1 \end{bmatrix}, \ddot{X}_{mp} = \begin{Bmatrix} \ddot{x}_0 \\ \ddot{y}_0 \\ \ddot{\theta} \end{Bmatrix} \tag{16}$$

The fast subsystem is obtained by ensuring that the slow variable is kept constant in the fast time scale, $h = (t - t_0)/\mu$ where t, t_0 and μ are a slow time scale, a slow initial time, and a perturbed parameter, respectively. Two variables, slow variable, v_s and fast variable, v_f are defined and related as $v_f = v - v_s$. After going through some derivations, the fast subsystem that represents transverse vibration [9] is yielded as

$$\hat{\hat{v}}_f(h) + A\hat{v}_f = F_{ff}(f_f), \tag{17}$$

where the initial conditions are $v_f(0) = v_{f0}$ and $\dot{v}_f(0) = v_{f1}$. $\hat{v}_f$ and $\hat{\hat{v}}_f$ are the first derivative and the second derivative, respectively, of the fast variable, v_f with respect to the fast time scale, h. F_{ff} is a 1×6 force transformation matrix in the transverse vibration, f_f is the interaction forces between a manipulator and the flexible beam, and A is a differential operator in Hilbert space.

4. Controller design

The singular perturbation technique is used to approximate solutions and reduce the order of the model of the system. From this method, two subsystems with different time scales are obtained: the slow and fast subsystems. A controller is designed for each subsystem that forms a composite controller. The slow subsystem represents the rigid body motion without involving any flexible parameters. It is used for trajectory tracking purposes. Thus, the controller is designed to move the flexible beam so that its midpoint's positions and orientation track the desired trajectories of the beam's midpoint. However, the fast subsystem represents the transverse vibration of the flexible beam. Hence, the controller is designed to suppress the beam's vibration in the fast subsystem.

The dynamics system of two cooperative manipulators handling the flexible beam is modeled by a set of coupled, highly non-linear differential equations. The controller design is not easy, although the system model is precisely known. In the practical operations of an industrial robot, since the mathematical model inevitably contains various uncertainties and disturbances, the widely used CTC scheme may not give a high precision performance [30]. FAT is needed to compensate for the uncertainties of the model. Therefore, adaptive approaches are used to formulate FATAC laws that can adequately track performance under various uncertainties for the slow subsystem. In contrast, VFC is used for the fast subsystem. The newly proposed composite controller for cooperative manipulators in handling the flexible beam is shown in Figure 3.

4.1. Fatac for the slow subsystem

The standard control design approach for the precisely known model may involve the singularity problem due to updating the inertia matrix. The singularity problem dramatically limits the effectiveness of the approach. Thus, a better approach [30] eliminates the requirement for acceleration feedback and avoids the singularity problem. A 3×1 error vector is defined as.

$$s = \dot{e} + \Lambda e \Rightarrow \dot{e} = s - \Lambda e \tag{18}$$

and its first derivative [30] is described as

$$\dot{s} = \ddot{e} + \Lambda\dot{e} \Rightarrow \ddot{e} = \dot{s} - \Lambda\dot{e} \tag{19}$$

where $\Lambda = diag(\lambda_1, \lambda_2, \ldots, \lambda_n)$ and $\lambda_n > 0$ for $i = 1, \ldots, n$. By this definition, a convergence, s implies the convergence of the 3×1 output error vector, e. The

system error [30] is given as

$$e = X_{mp} - X_{mpd} \tag{20}$$

where $X_{mp} \in \Re^{n\times 1}$ is the trajectory of the beam's midpoint and $X_{mpd} \in \Re^{n\times 1}$ is its desired trajectory. Differentiating equation (20) once and twice gives the first derivative and the second derivative of the error, respectively, [30] as

$$\dot{e} = \dot{X}_{mp} - \dot{X}_{mpd} \Rightarrow \dot{X}_{mp} = \dot{e} + \dot{X}_{mpd} \tag{21}$$

$$\ddot{e} = \ddot{X}_{mp} - \ddot{X}_{mpd} \Rightarrow \ddot{X}_{mp} = \ddot{e} + \ddot{X}_{mpd} \tag{22}$$

Then, substituting equations (18) and (19) into equations (21) and (22), respectively [30], gives

$$\dot{X}_{mp} = s - \Lambda e + \dot{X}_{mpd} \tag{23}$$

$$\ddot{X}_{mp} = \dot{s} - \Lambda \dot{e} + \ddot{X}_{mpd} \tag{24}$$

A new system model-based on the better approach [30] is obtained by substituting equations (18) and (19) as well as equations (23) and (24) into the equation (14) as

$$\begin{aligned} &M_{cr}(\dot{s} - \Lambda\dot{e} + \ddot{X}_{mpd}) + \\ &C_{cr}(s - \Lambda e + \dot{X}_{mpd}) + G_{cr} = U_{cr} \end{aligned} \tag{25}$$

Rewriting equation (25) becomes

$$\begin{aligned} &M_{cr}\dot{s} + C_{cr}s + G_{cr} + M_{cr}\ddot{X}_{mpd} - \\ &M_{cr}\Lambda\dot{e} + C_{cr}\dot{X}_{mpd} - C_{cr}\Lambda e = U_{cr} \end{aligned} \tag{26}$$

Suppose the system model is known precisely, and the control law for equation (26) is chosen as

$$\begin{aligned} U_{cr} = {} & M_{cr}\ddot{X}_{mpd} - M_{cr}\Lambda\dot{e} + \\ & C_{cr}\dot{X}_{mpd} - C_{cr}\Lambda e + G_{cr} - K_d s \end{aligned} \tag{27}$$

where K_d is a positive definite matrix. Hence, the closed-loop dynamics of the system are obtained by substituting equation (27) into equation (26) which yields

$$M_{cr}\dot{s} + C_{cr}s + K_d s = 0 \tag{28}$$

If the exact information of M_{cr}, C_{cr}, and G_{cr} is unavailable, then the control law in equation (27) cannot be realized. Thus, an adaptive control law is constructed according to equation (27) as

$$\begin{aligned} U_{cr} = {} & \hat{M}_{cr}\ddot{X}_{mpd} - \hat{M}_{cr}\Lambda\dot{e} + \hat{C}_{cr}\dot{X}_{mpd} - \\ & \hat{C}_{cr}\Lambda e + \hat{G}_{cr} - K_d s \end{aligned} \tag{29}$$

where $\hat{M}_{cr}$, $\hat{C}_{cr}$, and $\hat{G}_{cr}$ are the approximation of M_{cr}, C_{cr}, and G_{cr}, respectively. Defining a known signal vector as

$$v = \dot{X}_{mpd} - \Lambda e \tag{30}$$

and its first derivative as

$$\dot{v} = \ddot{X}_{mpd} - \Lambda\dot{e} \tag{31}$$

Substituting equations (30) and (31) into the control law of equation (29), the new form of control law without velocity feedback can be rewritten as

$$U_{cr} = \hat{M}_{cr}\dot{v} + \hat{C}_{cr}v + \hat{G}_{cr} - K_d s \tag{32}$$

Utilizing equation (32), the slow subsystem model of equation (26) can be written as

$$\begin{aligned} &M_{cr}\dot{s} + C_{cr}s + G_{cr} + \\ &M_{cr}(\ddot{X}_{mpd} - \Lambda\dot{e}) + C_{cr}(\dot{X}_{mpd} - \Lambda e) = U_{cr} \end{aligned} \tag{33}$$

The model can be obtained in terms of v and $\dot{v}$ by substituting equations (30) and (31) into equation (33)as

$$M_{cr}\dot{s} + C_{cr}s + G_{cr} + M_{cr}\dot{v} + C_{cr}v = U_{cr} \tag{34}$$

The closed-loop system can be obtained by substituting equation (32) into equation (34) as

$$M_{cr}\dot{s} + C_{cr}s + K_d s = -\tilde{M}_{cr}\dot{v} - \tilde{C}_{cr}v - \tilde{G}_{cr} \tag{35}$$

where $\tilde{M}$is the estimation error defined by

$$\begin{aligned} \tilde{M}_{cr} &= M_{cr} - \hat{M}_{cr}, \\ \tilde{C}_{cr} &= C_{cr} - \hat{C}_{cr}, \\ \tilde{G}_{cr} &= G_{cr} - \hat{G}_{cr}. \end{aligned} \tag{36}$$

The regressor-free adaptive controller can be designed using FAT to approximate the model of two cooperative manipulators handling a flexible beam. FAT is used to represent M_{cr}, C_{cr}, and G_{cr} with the assumption that the proper number of basis functions are employed [30] as

$$\begin{aligned} M_{cr} &= W_M^T Z_M + \varepsilon_M, \\ C_{cr} &= W_C^T Z_C + \varepsilon_C, \\ G_{cr} &= W_G^T Z_G + \varepsilon_G, \end{aligned} \tag{37}$$

where $W_M \in \Re^{n^2\beta_M\times n}$, $W_C \in \Re^{n^2\beta_C\times n}$, and $W_G \in \Re^{n^2\beta_G\times n}$ denote weighting matrices while $Z_M \in \Re^{n^2\beta_M\times n}$, $Z_C \in \Re^{n^2\beta_C\times n}$, and $Z_G \in \Re^{n^2\beta_G\times 1}$ represent matrices of basis functions. The number $\beta_{(.)}$ represents the number of basis functions and $\varepsilon_{(.)}$ represents approximation error matrices that are assumed to be zero in this study. Using the same set of basis functions, the corresponding estimates can be described [30] as

$$\begin{aligned} \hat{M}_{cr} &= \hat{W}_M^T Z_M, \\ \hat{C}_{cr} &= \hat{W}_C^T Z_C, \\ \hat{G}_{cr} &= \hat{W}_G^T Z_G. \end{aligned} \tag{38}$$

Using equation (37), the model of equation (34) becomes the FAT-based model [30] as

$$\begin{aligned} &M_{cr}\dot{s} + C_{cr}s + W_G^T Z_G + W_M^T Z_M\dot{v} + \\ &W_C^T Z_C v = U_{cr} \end{aligned} \tag{39}$$

Substituting equation (38) into the control law of equation (32) to obtain FAT-based control law [30] as

$$U_{cr} = \hat{W}_M^T Z_M\dot{v} + \hat{W}_C^T Z_C v + \hat{W}_G^T Z_G - K_d s \tag{40}$$

Then, the closed-loop system is obtained by substituting the FAT-based control law of equation (40) into a

FAT-based model of equation (39) as

$$M_{cr}\dot{s} + C_{cr}s + K_d s = -\tilde{W}_M^T Z_M \dot{v} - \tilde{W}_C^T Z_C v - \tilde{W}_G^T Z_G \tag{41}$$

where

$$\begin{aligned} \tilde{W}_M &= W_M - \hat{W}_M, \\ \tilde{W}_C &= W_C - \hat{W}_C, \\ \tilde{W}_G &= W_G - \hat{W}_G, \end{aligned} \tag{42}$$

and its derivatives [30] become

$$\begin{aligned} \dot{\tilde{W}}_M &= -\dot{\hat{W}}_M, \\ \dot{\tilde{W}}_C &= -\dot{\hat{W}}_C, \\ \dot{\tilde{W}}_G &= -\dot{\hat{W}}_G. \end{aligned} \tag{43}$$

Rewriting equation (41) [30] becomes

$$\dot{s} = {M_{cr}}^{-1} \begin{pmatrix} -C_{cr}s - K_d s - \tilde{W}_M^T Z_M \dot{v} \\ -\tilde{W}_C^T Z_C v - \tilde{W}_G^T Z_G \end{pmatrix} \tag{44}$$

4.1.1. Lyapunov stability analysis

A Lyapunov stability theory is used to design controllers that stabilize a non-linear system of two cooperative manipulators handling the flexible object. Since $W_{(.)}$ is a constant vector, their update laws can be easily found by adequately selecting the Lyapunov-like function. A Lyapunov candidate [30] is considered as

$$V(s, \tilde{W}_M, \tilde{W}_C, \tilde{W}_G) = \frac{1}{2}s^T M_{cr} s + \frac{1}{2} Tr(\tilde{W}_M^T Q_M \tilde{W}_M + \tilde{W}_C^T Q_C \tilde{W}_C + \tilde{W}_G^T Q_G \tilde{W}_G) \tag{45}$$

where $\mathcal{Q}_M \in \Re^{n^2\beta_M \times n^2\beta_M}$, $\mathcal{Q}_C \in \Re^{n^2\beta_C \times n^2\beta_C}$, and $\mathcal{Q}_G \in \Re^{n\beta_G \times n\beta_G}$ are positive definite weighting matrices, $\beta_{(.)}$ represents the number of basis functions, and Tr is the trace of matrices. The time derivative of V as equation (41) [30] can be computed as

$$\dot{V} = s^T M_{cr}\dot{s} + \frac{1}{2}s^T \dot{M}_{cr} s + Tr(\tilde{W}_M^T Q_M \dot{\tilde{W}}_M + \tilde{W}_C^T Q_C \dot{\tilde{W}}_C + \tilde{W}_G^T Q_G \dot{\tilde{W}}_G) \tag{46}$$

Substituting equation (44) into equation (46) [30] gives

$$\dot{V} = s^T M_{cr} {M_{cr}}^{-1} \begin{pmatrix} -C_{cr}s - K_d s - \tilde{W}_M^T Z_M \dot{v} \\ -\tilde{W}_C^T Z_C v - \tilde{W}_G^T Z_G \end{pmatrix} + \frac{1}{2}s^T \dot{M}_{cr} s + Tr \begin{pmatrix} \tilde{W}_M^T Q_M \dot{\tilde{W}}_M \\ +\tilde{W}_C^T Q_C \dot{\tilde{W}}_C + \tilde{W}_G^T Q_G \dot{\tilde{W}}_G \end{pmatrix} \tag{47}$$

Rearranging equation (47) becomes

$$\begin{aligned} \dot{V} = -s^T K_d s + \left[\frac{1}{2}s^T \dot{M}_{cr} s - s^T C_{cr} s\right] \\ - [s^T \tilde{W}_M^T Z_M \dot{v} - Tr(\tilde{W}_M^T Q_M \dot{\tilde{W}}_M)] \\ - [s^T \tilde{W}_C^T Z_C v - Tr(\tilde{W}_C^T Q_C \dot{\tilde{W}}_C)] \\ - [s^T \tilde{W}_G^T Z_G - Tr(\tilde{W}_G^T Q_G \dot{\tilde{W}}_G)] \end{aligned} \tag{48}$$

Then, simplifying equation (48) by using equation (43) gives

$$\begin{aligned} \dot{V} = -s^T K_d s + \left[\frac{1}{2}s^T \dot{M}_{cr} s - s^T C_{cr} s\right] \\ - [s^T \tilde{W}_M^T Z_M \dot{v} + Tr(\tilde{W}_M^T Q_M \dot{\hat{W}}_M)] \\ - [s^T \tilde{W}_C^T Z_C v + Tr(\tilde{W}_C^T Q_C \dot{\hat{W}}_C)] \\ - [s^T \tilde{W}_G^T Z_G + Tr(\tilde{W}_G^T Q_G \dot{\hat{W}}_G)] \end{aligned} \tag{49}$$

$$\begin{aligned} \dot{V} = -s^T K_d s + \left[\frac{1}{2}s^T (\dot{M}_{cr} - 2C_{cr}) s\right] \\ - Tr[\tilde{W}_M^T (Z_M \dot{v} s^T + Q_M \dot{\hat{W}}_M)] \\ - Tr[\tilde{W}_C^T (Z_C v s^T + Q_C \dot{\hat{W}}_C)] \\ - Tr[\tilde{W}_G^T (Z_G s^T + Q_G \dot{\hat{W}}_G)] \end{aligned} \tag{50}$$

Since the matrix $\dot{M}_{cr} - 2C_{cr}$ is a skew-symmetric [30], the update laws are selected from equation (50) to be

$$\begin{aligned} \dot{\hat{W}}_M &= {Q_M}^{-1} Z_M \dot{v} s^T, \\ \dot{\hat{W}}_C &= {Q_C}^{-1} Z_C v s^T, \\ \dot{\hat{W}}_G &= {Q_G}^{-1} Z_G s^T, \end{aligned} \tag{51}$$

so that $\dot{V} = -s^T K_d s \leq 0$. Since $V > 0$, $\dot{V} \leq 0$. Therefore, $s(t) \to 0$ and $e \to 0$ as $t \to \infty$ based on Barbalat Lemma.

4.2. Vfc for the fast subsystem

A VFC is used to suppress the beam's vibration in the fast subsystem because of its simple implementation in real-time, a limited number of sensor requirements, and irrespective of boundary conditions [9]. The controller is used with either the CTC scheme or the FATAC to make up the composite controller controlling the complete cooperative manipulators and flexible beam system. The objective of the controller is to damp out the deflection of the flexible beam by utilizing the following velocity feedback control law.

$$U_f = (f_f) = -\Phi F_{ff}^{\dagger} \hat{v}_f(h) \tag{52}$$

where $F_{ff}^{\dagger}$ is the pseudo-inverse of F_{ff} [9]. The operator $\Phi = K\Omega\lambda$ is neither a self-adjoint nor a positive definite, where K is the positive gain, $\Omega = \lambda^{\sigma}$ is a bounded and positive definite operator with $\sigma = -1/2$, and λ is a positive definite operator [21] and [31]. Further explanation of the stability analysis of the fast control can be found in [9].

5. Simulation results

For the closed-loop control system simulations, the slow subsystem in equation (14) is incorporated with

Table 1. Control parameters for the FATAC.

Parameter	Value
T	20 s
Λ	diag (20 20 20)
K_d	diag (500 900 500)
Q_M	⋮
Q_C	⋮
Q_G	⋮

the FATAC in equation (40). The manipulators are commanded to move the flexible beam so that its midpoint's position and orientation, X_{mp} track desired trajectories of the beam's midpoint, X_{mpd} as

$$X_{mpd} = \begin{bmatrix} x_{od} & y_{od} & \theta_d \end{bmatrix}^T \tag{53}$$

where $x_{od} = 0.1\sin(t)$ is the desired X-position, $y_{od} = 0.1\cos(t) + 0.1$ is the desired Y-position, and $\theta_d = 0$ is the desired orientation of the beam, while t is the time taken for simulation or hardware experimental tests.

The initial positions and the orientation of the beam's midpoint are set as $X_{mp} = \{0\text{ m}, 0\text{ m}, 0.1\text{ rad}\}^{\mathrm{T}}$ meanwhile, the initial velocity, $\dot{X}_{mp}$ and acceleration, $\ddot{X}_{mp}$ are considered as zero. The distance between two manipulators' bases is 1 m apart. The simulations have been carried out using ode2 typed into the solver in MATLAB Simulink with a sampling period of 0.001 s and a simulation time of 10 s. The number of basis functions is considered according to the trial-and-error method. The performance tracking is poor when a low number of basis functions is chosen and vice versa. However, the computational time will increase when a higher number of basis functions is determined. The number of basis functions is set as 10 in this simulation. The controller parameters for the FATAC are presented in Table 1.

The control signal produced by the FATAC is shown in Figure 4, Figure 5 and Figure 6 to track the desired X-position, Y-position, and orientation, respectively. It can be seen that the RMS values of the controller output in the form of torque produced by the FATAC are 5.851, 31.28, and 11.94 N.m for X-direction, Y-direction, and the orientation, respectively. It also can be observed that the control signals have large spikes for some time in some instances due to derivative terms in control law (40), and no filter is used in this simulation. However, the spikes do not affect the trajectory tracking, as depicted in Figure 7, Figure 8 and Figure 9. It is suggested that a low pass filter can be used to filter out the spikes from the controller signals if it gives a severe problem when implementing experimental hardware tests later.

The tracking of planar motions of the beam's midpoint along the X-direction, Y-direction, and the orientation by using the proposed FATAC are shown in Figure 7, Figure 8 and Figure 9, respectively. The tracking errors of the beam's midpoint, X_{mp} using the proposed FATAC, are shown in Figure 10 and its trace

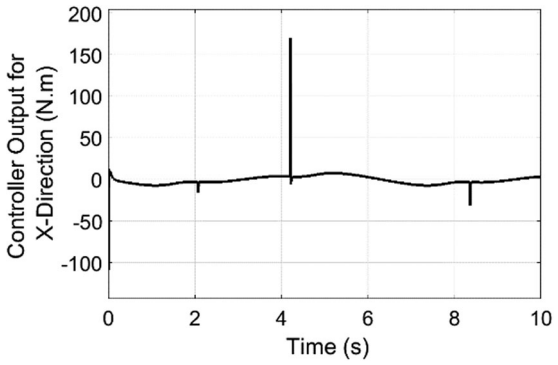

Figure 4. Controller signal of the FATAC in the X-direction.

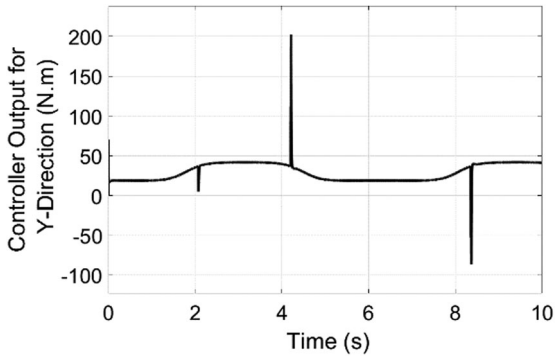

Figure 5. Controller signal of the FATAC in the Y-direction.

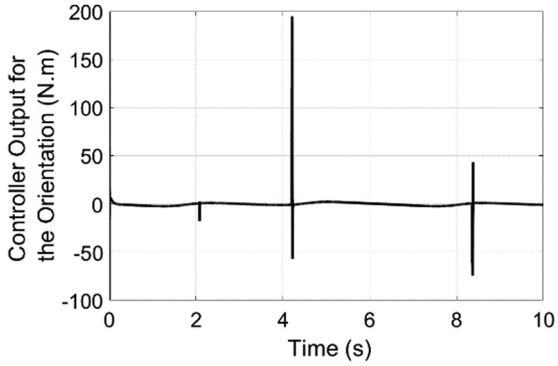

Figure 6. Controller signal of the FATAC for the orientation.

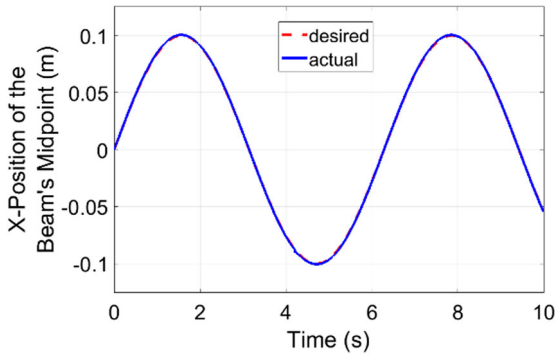

Figure 7. X-position tracking of the beam's midpoint using the proposed FATAC.

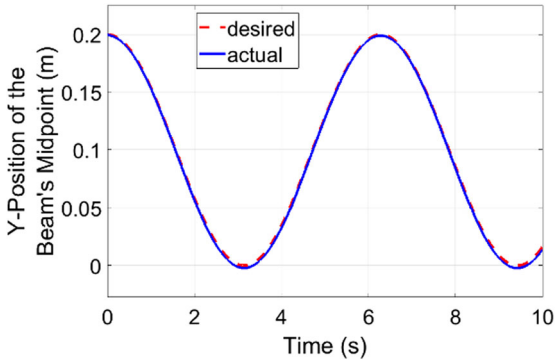

Figure 8. Y-position tracking of the beam's midpoint using the proposed FATAC.

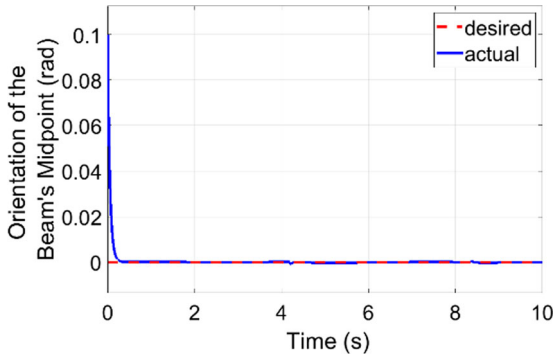

Figure 9. Orientation tracking of the beam's midpoint using the proposed FATAC.

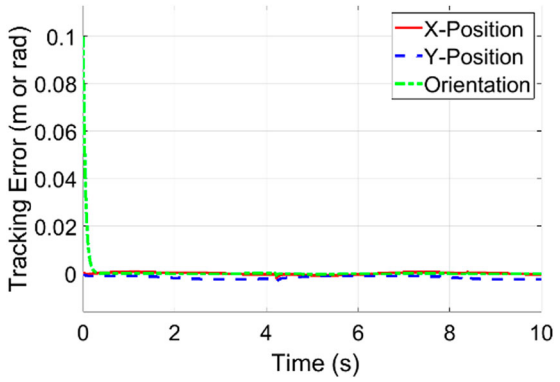

Figure 10. Tracking errors of the beam's midpoint using the proposed FATAC.

Table 2. RMSE values for simulation of the proposed FATAC.

Positions/Orientation	Value
X-direction	4.599e-3 m
Y-direction	1.697e-3 m
Orientation	5.186e-3 rad

in the XY-plane is shown in Figure 11. It can be observed that the position tracking and the orientation under the proposed FATAC is successfully achieved with root-mean-square error (RMSE) values of 4.599e-3 m, 1.697e-3 m, and 5.186e-3 rad for X-direction, Y-direction, and the orientation, respectively, as shown in Table 2.

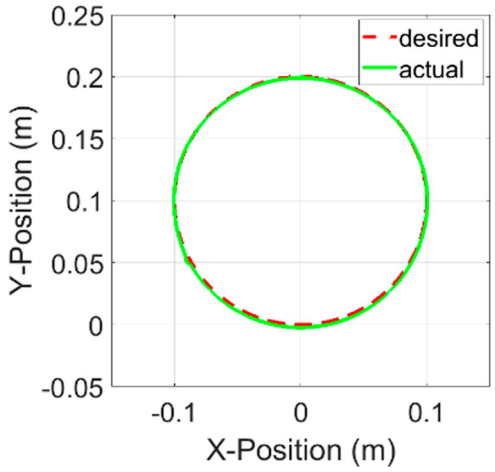

Figure 11. Trace of the beam midpoint in the XY-plane using the proposed FATAC.

Table 3. RMSE values for simulation of the CTC scheme.

Positions/Orientation	Value
X-direction	2.745e-3 m
Y-direction	2.292e-2 m
Orientation	1.563e-2 rad

The simulation results under the proposed FATAC can be compared to those using the CTC scheme [26]. The simulation results under the CTC scheme showed that the position tracking and the orientation had been achieved with the RMSE values of 2.745e-3 m, 2.292e-2 m, and 1.563e-2 rad for X-direction, Y-direction, and the orientation, respectively, as depicted in.

Table 3. These results showed that the RMSE values of Y-direction and the orientation for the proposed FATAC have smaller values than the CTC scheme. For X-direction, the RMSE value of the proposed FATAC has a slightly higher value than the CTC scheme. These results proved that the proposed FATAC is more accurate in trajectory tracking than the CTC scheme. The proposed FATAC has also successfully driven the cooperative manipulators to handle the flexible beam so that it follows the desired trajectory.

The fast subsystem model in the equation (17) is incorporated with VFC law in the equation (52). The simulation has considered the initial disturbance of 5 mm with zero initial velocity. The control parameters of λ and K are chosen as diag {80} and 1, respectively. With the value of $\sigma = -1/2$, the beam's transverse vibration is completely suppressed at around 0.8 s, as shown in Figure 12. The results proved that the proposed VFC for the fast subsystem has successfully suppressed the beam's vibration.

6. Hardware experimental set-up

The proposed controllers will be validated through experimental hardware tests to manipulate the flexible

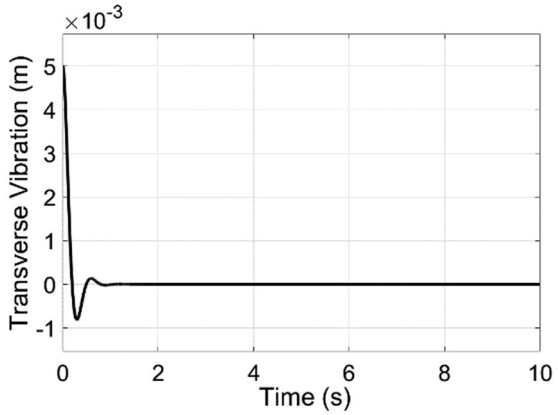

Figure 12. Suppression of the beam's vibration using the VFC.

beam according to the desired trajectory while suppressing its vibration. The hardware set-up of the system consists of a pair of three-links and planar manipulators, the flexible beam, and a computer with the installed LabVIEW software, as shown in Figure 13. Each manipulator consists of hardware components as follows:

(1) Three rigid links are fabricated by using stainless steel.
(2) Three direct current (DC) planet geared motors with the model number 1403190008 manufactured by Ningbo Twirl Motor Co. Ltd.
(3) Two motor drivers from Cytron Technologies drive motors in each manipulator. The Model MDDS10 DC motor driver drives motors 1 and 2. Model MD10C DC motor drives motor 3
(4) A data acquisition (DAQ) device from National Instrument (NI-DAQmx USB-6211) is used to communicate between the computer and the manipulator, such as reading the sensors and running the motors. It has 16 analog inputs that are denoted as ai0, ai1, ai2 up to ai15, two analog outputs that are represented as ao0 and ao1, four digital inputs that are designated as PFI 0, PFI 1, PFI 2, and PFI 3, four digital outputs that are denoted as PFI4, 71 PFI 5, PFI 6 and PFI 7, and two 32-bit counters.
(5) Six proximity sensors are used as limit sensors and located at each link to provide the safe movement of each link.
(6) Three hall effect sensors from Vishay (Model 981 HE) are coupled with three motors to measure the angular displacement of joints.
(7) An emergency button is provided for safety and precaution while running the cooperative manipulators.

The flexible beam is cemented with a strain gauge sensor, and two connectors are used to attach the flexible beam to cooperative manipulators, as shown in Figure 14. The strain gauge sensor is used to measure the vibration. However, it gives the reading in voltage that needs calibration to provide the reading in the unit of length, which is a millimeter (mm). The calibration process is also done to ensure that the strain gauge sensor works well in preparation for experimental hardware tests. Then, the program coding of the controller for each subsystem is developed using the LabVIEW platform and verified through experimental hardware tests.

For the slow subsystem, two cooperative manipulators are controlled using the proposed FATAC so that the positions and the orientation of the beam's midpoint track the desired trajectory. The desired circular trajectory of the beam's midpoint is considered with a

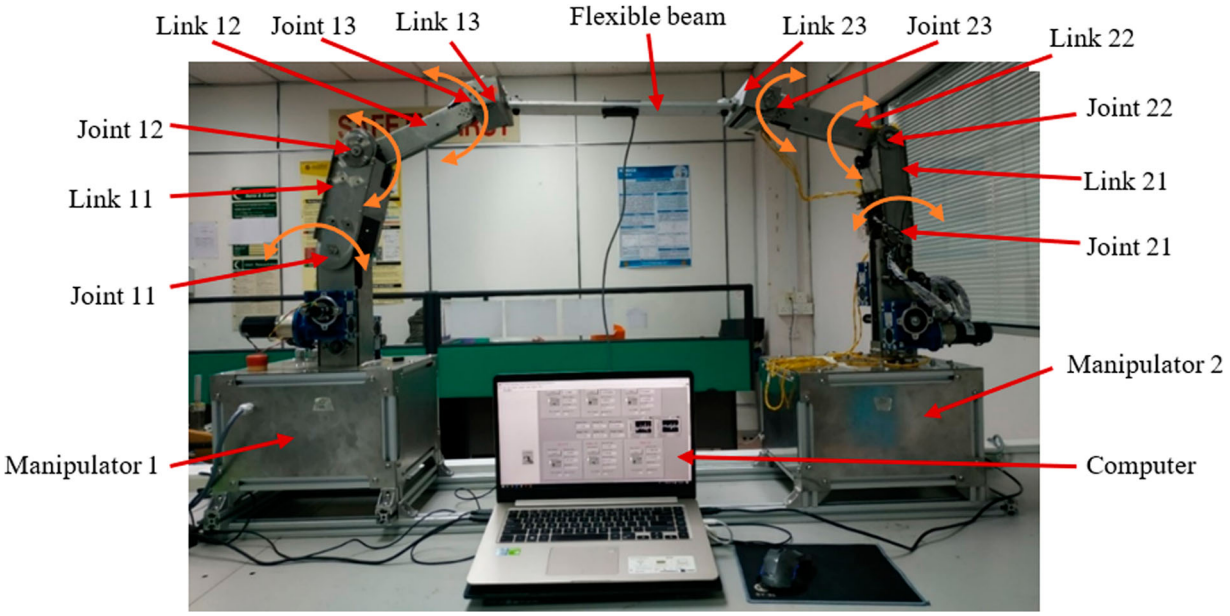

Figure 13. Experimental set-up of the system.

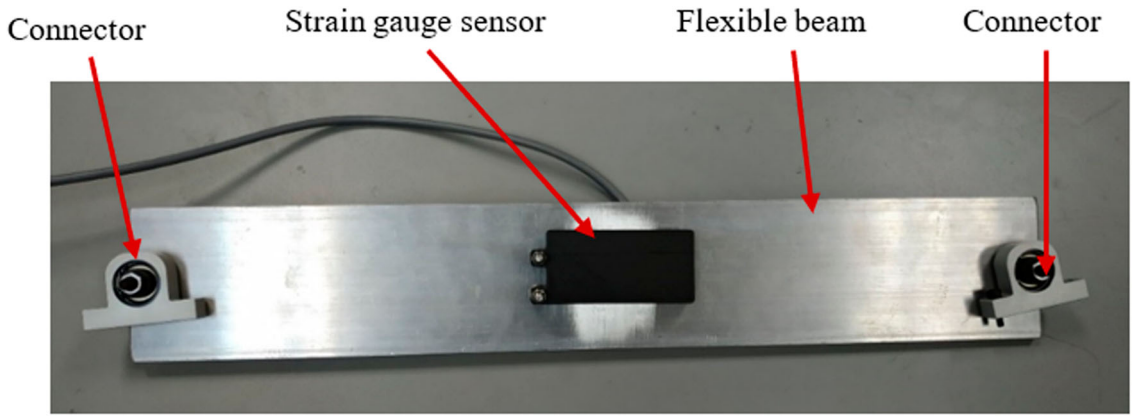

Figure 14. Experimental set-up for the flexible beam.

Table 4. Control parameters of Manipulator 1 for controlling the beam's midpoint to track the desired trajectory using the proposed FATAC.

Parameter	Value
T	20 s
Λ	diag (28 28 28)
K_d	diag (1.1 1.1 1.1)
Q_M	1000**I**
Q_C	1000**I**
Q_G	1000**I**

Table 5. Control parameters of Manipulator 2 for controlling the beam's midpoint to track the desired trajectory using the proposed FATAC.

Parameter	Value
T	20 s
Λ	diag (27 28 28)
K_d	diag (0.7 0.7 3.7)
Q_M	1000**I**
Q_C	1000**I**
Q_G	1000**I**

radius of 10 cm and the center point at (58, 20 cm). The length of each link for both manipulators is 21.0 cm for link 1, 27.5 cm for link 2, and 5.0 cm for link 3. The actual length of the beam is 48.6 cm. In Cartesian space, the base of Manipulator 1 is considered as the origin at (0, 0 cm), while the base of Manipulator 2 is at (116.7, 0 cm). Configurations of the manipulators are elbow-up for Manipulator 1 and elbow-down for Manipulator 2.

The beam's midpoint is initially positioned at (58.0, 10.0 cm), which gives initial joint angles of Manipulator 1, 1.438 rad. for joint 1, 0.340 rad. for joint 2, and −0.341 rad. for joint 3; and initial joint angles of Manipulator 2 which are 1.739 rad. for joint 1, 2.797 rad. for joint 2, and 0.345 rad. for joint 3. The experimental hardware tests are carried out for 2000ms. The number of the basis functions is considered according to the trial-and-error method. Like simulation, the number of basis functions is set as 10 in this experimental hardware test. All control parameters used in experimental hardware tests of the proposed FATAC for two cooperative manipulators in handling the beam's midpoint so that it tracks the circular desired trajectory are presented in Table 4 and Table 5 for Manipulator 1 and Manipulator 2, respectively.

7. Hardware experimental tEST results

The tracking motions of the beam's midpoint consist of X-position, Y-position, and orientation by using the proposed FATAC as the results of experimental hardware tests, as shown in Figure 15, Figure 16 and Figure 17. In contrast, their tracking errors are shown

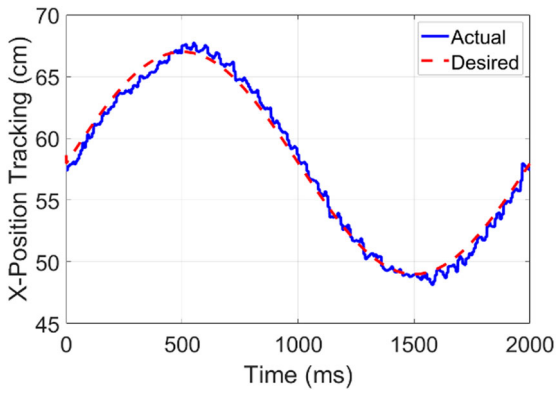

Figure 15. X-position tracking of the beam's midpoint using the proposed FATAC.

in Figure 18. The motion's trace of the beam's midpoint in the XY-plane is illustrated in Figure 19. The motion's tracking of the beam's midpoint can be accomplished by controlling the motor at each joint of both manipulators, as shown in Figure 20, Figure 21, Figure 22, Figure 23, Figure 24 and Figure 25. It can be observed that the tracking of the beam's midpoint, which is controlled by two cooperative manipulators using the proposed FATAC, has been successfully achieved with the RMSE values, as shown in Table 6. The experimental results proved that the proposed FATAC has successfully driven the experimental hardware of two cooperative manipulators in controlling the beam's midpoint to follow the desired trajectory.

The results contain noisy signals due to the mechanical issues on joint 2 of robot manipulator 2, which

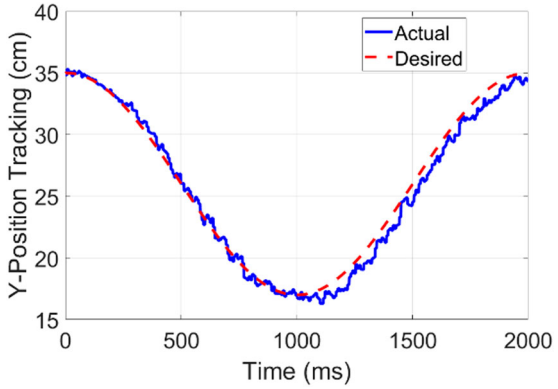

Figure 16. Y-position tracking of the beam's midpoint using the proposed FATAC.

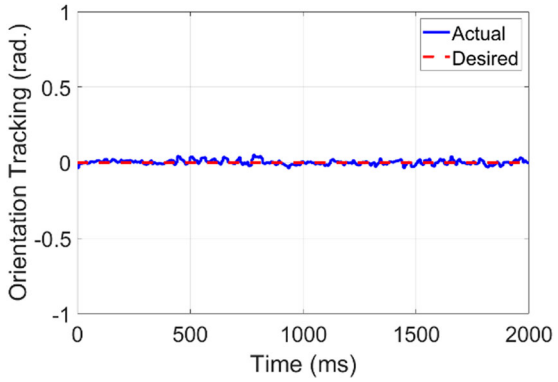

Figure 17. Orientation tracking of the beam's midpoint using the proposed FATAC.

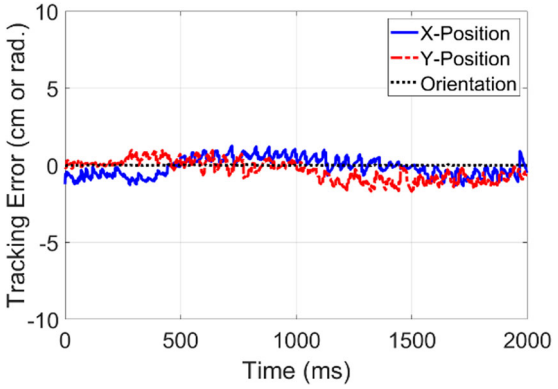

Figure 18. Tracking error of the beam's midpoint using the proposed FATAC.

Table 6. RMSE values for experimental hardware tests of the proposed FATAC.

Positions/Orientation	Value
X-direction	6.108e-3 m
Y-direction	7.392e-3 m
Orientation	1.510e-2 rad

has a backlash that caused link 2 to shake during the movement. The robot manipulators, including all the links, are fabricated using the stainless steel. Each robot manipulator is designed in which a metal chain is used at joint 1 that helps to move link 1 by motor 1 and

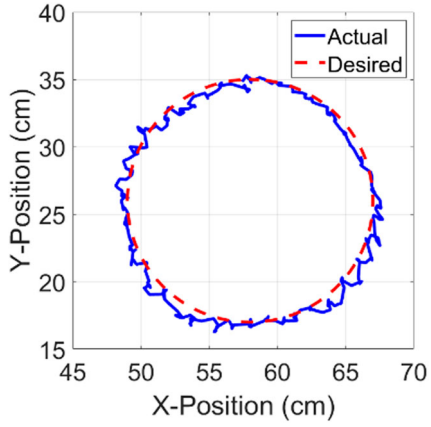

Figure 19. Trace of the beam's midpoint in the XY-plane using the proposed FATAC.

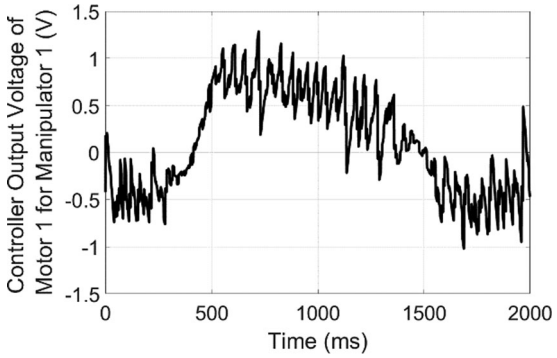

Figure 20. Controller signal to the motor at the Joint 1 of Manipulator 1.

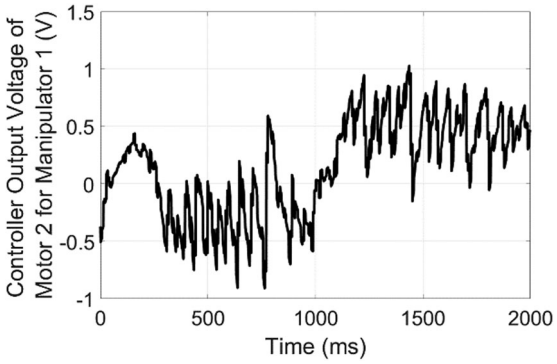

Figure 21. Controller signal to the motor at the Joint 2 of Manipulator 1.

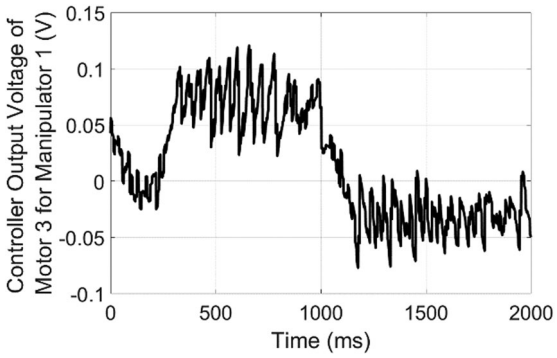

Figure 22. Controller signal to the motor at the Joint 3 of Manipulator 1.

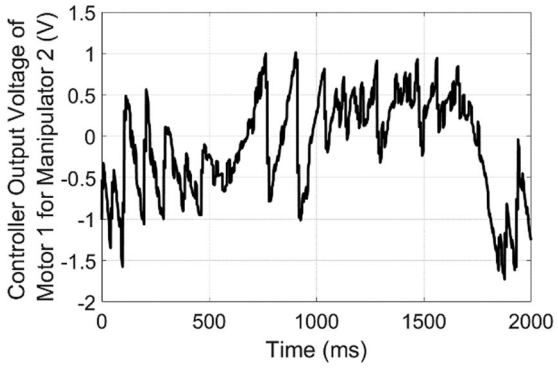

Figure 23. Controller signal to the motor at the Joint 1 of Manipulator 2.

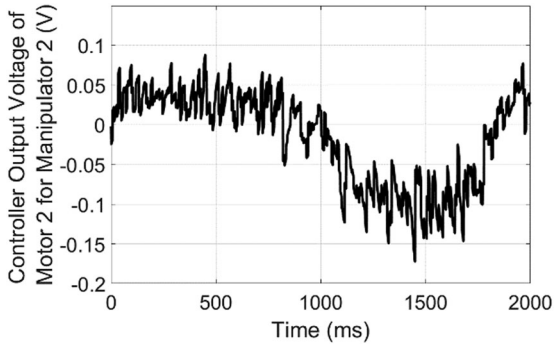

Figure 24. Controller signal to the motor at the Joint 2 of Manipulator 2.

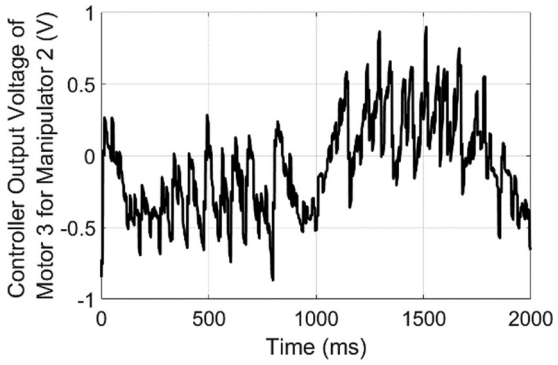

Figure 25. Controller signal to the motor at the Joint 3 of Manipulator 2.

joint 2, which allows link 2 by motor 2. A motor is also installed at joint 3 in each robot manipulator to control link 3 directly. The mechanical design and the heavy material led to a backlash, mechanical shaking during the movement, and noisy signal of the trajectory tracking. In the future, trajectory tracking can be improved by enhancing the mechanical design and proper tuning. The robot manipulators should be fabricated using a lighter material, choosing smaller and lighter motors and ensuring the chain is tight to avoid backlash.

For the fast subsystem, VFC is proposed to suppress the vibration of the flexible beam. The control parameters of λ, K, and σ are chosen as diag {50}, 3, and $-1/2$, respectively. The experimental result of the beam's vibration during its movement by two cooperative

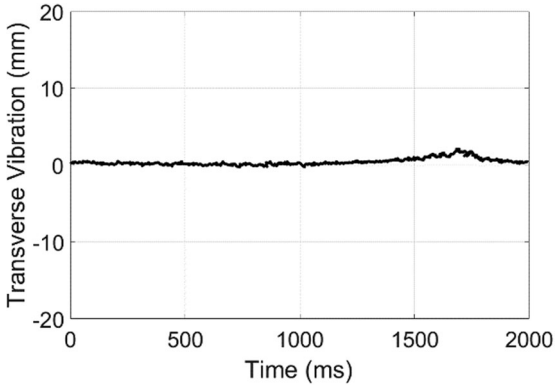

Figure 26. Suppression of the beam's vibration using VFC.

manipulators is shown in Figure 26. The experimental results proved that the proposed VFC for the fast subsystem has successfully suppressed the beam vibration. At the same time, the cooperative manipulators move the flexible beam according to the desired trajectory. Note that the beam's orientation in this paper has been changed to 0.1 rad due to the singularity problem.

8. Conclusion

This paper proposes a composite controller for a closed-loop system comprising the FATAC and the VFC for two three-links and planar cooperative manipulators to handle the flexible beam, track the desired trajectory, and suppress the beam's vibration. The mathematical modeling has been presented based on the extended Hamiltonian technique. As a result, two subsystems, namely the slow and fast subsystems, of the singular perturbation model with different time scales are obtained and presented in the PDE form. Each subsystem model is constructed by using Simulink for simulation purposes. Simulation tests have been carried out to measure the proposed controller's performance. For the slow subsystem, the simulation results showed that the RMSE values of positions and the orientation of the beam's midpoint using the proposed FATAC are 4.599e-3 m, 1.697e-3 m, and 5.186e-3 rad for X-direction, Y-direction, and the orientation, respectively. The simulation results under the proposed FATAC can be compared to those using the CTC scheme [26]. The simulation results under the CTC scheme showed that the tracking of positions and orientation had been achieved with the RMSE values of 2.745e-3 m, 2.292e-2 m, and 1.563e-2 rad for X-direction, Y-direction, and orientation, respectively. These results showed that the RMSE values of Y-direction and the orientation for the proposed FATAC have smaller values than the CTC scheme. For X-direction, the RMSE of the proposed FATAC has a slightly higher value than the CTC scheme. These results proved that the proposed FATAC is more accurate in trajectory tracking than the CTC scheme. The proposed FATAC has also successfully driven the cooperative manipulators

to handle the flexible beam to follow the desired trajectory. For the experimental hardware tests, the coding of the proposed FATAC is developed to control two cooperative manipulators so that the positions of the beam's midpoint track the circular desired trajectory. It can be observed that the position tracking of the beam's midpoint, controlled by two cooperative manipulators under the proposed FATAC, has been successfully achieved with the RMSE values of 6.108e-3 m for X-position, 7.392e-3 m for Y-position, and 1.510e-2 rad for the orientation. These results proved that the proposed FATAC for the slow subsystem has successfully driven the experimental hardware of two cooperative manipulators in controlling the beam's midpoint to follow the desired trajectory. For the fast subsystem, VFC has been validated by experimental hardware tests to suppress the vibration of the flexible beam. The experimental results proved that the proposed VFC has successfully suppressed the beam vibration while moving the flexible beam to follow the desired trajectory. Several contributions of this research are (1) the proposed controller caters to the model uncertainty problem, (2) the proposed controller does not require the knowledge of the precise model, and (3) the proposed controller does not use the regressor matrix that is highly computation, (4) the proposed controller is easy to be programmed for experimental hardware tests, and (5) the research presents the experimental works on the control of cooperative manipulators in handling deformable objects. In the future, the research can be extended to higher DOF robots, the control laws can be tested for other types of deformable objects, and the hardware used in the experiment can be improvised.

Disclosure statement

No potential conflict of interest was reported by the author(s).

Funding

This work was supported by TWAS COMSTECH: [Grant Number 15-321 RG/ENG/AS_C-FR3240288945].

References

[1] Zheng YF, Chen MZ. Trajectory planning for two manipulators to deform flexible beams. Robot Auton Syst. 1994;12:55–67. doi:10.1016/0921-8890(94)90046-9

[2] AlYahmadi AS, Hsia TC. Internal force-based impedance control of dual-arm manipulation of flexible objects. Proc 2000 IEEE Intern Confer Robot Autom. 2000;4:3296–3301. doi:10.1109/ROBOT.2000.845171

[3] Doulgeri Z, Peltekis J. Modeling and dual arm manipulation of a flexible object. Proc 2004 IEEE Int Conf Robot Autom. 2004;April:1700–1705. doi:10.1109/ROBOT.2004.1308069

[4] Long P, Khalil W, Martinet P. Dynamic modeling of cooperative robots holding flexible objects. 2015 International Conference on Advanced Robotics (ICAR). 2015:182–187. doi:10.1109/ICAR.2015.7251453

[5] Tang Z, Li Y. Modeling and control of two manipulators handling a flexible payload based on singular perturbation. 2010 2nd International Conference on Advanced Computer Control. 2010;vol. 1:558–562. doi:10.1109/ICACC.2010.5487171

[6] Ji Y, Park Y. Optimal input design for a cooperating robot to reduce vibration when carrying flexible objects. Robotica. 2001;19:209–215. doi:10.1017/S0263574700002915

[7] Al-Yahmadi AS, Abdo J, Hsia TC. Modeling and control of two manipulators handling a flexible object. J Franklin Inst. 2007;344:349–361. doi:10.1016/j.jfranklin.2006.01.002

[8] Tavasoli A, Eghtesad M, Jafarian H. Two-time scale control and observer design for trajectory tracking of two cooperating robot manipulators moving a flexible beam. Rob Auton Syst. 2009;57(2):212–221. doi:10.1016/j.robot.2008.04.003

[9] Esakki B, Bhat RB, Su C-Y. Robust control of collaborative manipulators - flexible object system. International Journal of Advanced Robotic Systems. 2013;10(257). doi:10.5772/56204

[10] Dou H, Wang S. A boundary control for motion synchronization of a two-manipulator system with a flexible beam. Automatica (Oxf). 2014;50(12):3088–3099. doi:10.1016/j.automatica.2014.10.057

[11] Liu Z, Liu J. Adaptive iterative learning boundary control of a flexible manipulator with guaranteed transient performance. Asian J Contr. 2018;20(3):1027–1038. doi:10.1002/asjc.1379

[12] Ashayeri A, Eghtesad M, Farid M, et al. Two-time scale fuzzy logic controller and observer design for trajectory tracking of two cooperating robot manipulators handling a flexible beam. EUROCON 2007 - The International Conference on "Computer as a Tool". 2007;57(2):745–752. doi:10.1109/EURCON.2007.4400286

[13] Liu S, Li Y, Langari R. Force control of dual-manipulator handling a flexible payload based on distributed parameter model. 2018 Chinese Automation Congress (CAC). 2018: 2820–2824. doi:10.1109/CAC.2018.8623574

[14] Navarro-Alarcon D, Liu Y-H, Romero JG, et al. Model-free visually servoed deformation control of elastic objects by robot manipulators. IEEE Trans Robot. 2013;29(6):1457–1468. doi:10.1109/TRO.2013.2275651

[15] Berenson D. Manipulation of deformable objects without modeling and simulating deformation. 2013 IEEE/RSJ International Conference on Intelligent Robots and Systems. 2013: 4525–4532. doi:10.1109/IROS.2013.6697007

[16] Jasim IF, Plapper PW, Voos H. Model-Free Robust Adaptive Control for flexible rubber objects manipulation. In IEEE International Conference on Emerging Technologies and Factory Automation, ETFA. 2015;2015-Octob:0–7.

[17] Spong MW, Hutchinson S, Vidyasagar M. Robot modeling and control. IEEE Contr Syst. 2006;26(6):113–115. doi:10.1109/MCS.2006.252815

[18] Sun D, Liu Y. Modeling and impedance control of a two-manipulator system handling a flexible beam. ASME J Dyn Syst Meas Contr. 1997;119(April):736–742. doi:10.1115/1.2802385

[19] Liu Y, Sun D. Stabilizing a flexible beam handled by two manipulators via PD feedback. IEEE Trans Autom Contr. 2000;45(11):2159–2164. doi:10.1109/9.887656

[20] Sun D, Liu Y. Position and force tracking of a Two-manipulator system manipulating a flexible beam payload. In Proceedings of the 2001 IEEE International Conference on Robotics and Automation. 2001: 3483–3488.
[21] Luo ZH. Direct strain feedback control of flexible robot arms: new theoretical and experimental results. IEEE Trans Automat Contr. 1993;38(11):1610–1622. doi:10.1109/9.262031
[22] He W, Ge SS. Vibration control of a flexible beam with output constraint. IEEE Trans Ind Electron. 2015;62(8):5023–5030. doi:10.1109/TIE.2015.2400427
[23] Lee AX, Lu H, Gupta AAA, et al. Learning force-based manipulation of deformable objects from multiple demonstrations, In Proc. - IEEE Int. Conf. Robot. Autom., vol. 2015-June, no. June, pp. 177–184, 2015.
[24] Esakki B, Ahmed SR. Dynamics and control of collaborative robot manipulators. In 2015 International Conference on Smart Technologies and Management for Computing, Communication, Controls, Energy and Materials. 2015: 590–595.
[25] Samewoi AR, Azlan NZ, Khan MR. Kinematics analysis and trajectory validation of two cooperative manipulators handling a flexible beam. In 7th IEEE International Conference on Mechatronics Engineering. 2020.
[26] Samewoi AR, Azlan NZ, Khan MR, et al. Computed torque and velocity feedback control of cooperative manipulators handling a flexible beam. International Journal of Nanoelectronics & Materials. 2020;13(Special Issue ISSTE 2019):17–34.
[27] Landau ID, Lozano R, M'Saad M, et al. Adaptive control : algorithms, analysis and applications. London: Springer; 2011.
[28] Zribi M, Karkoub M, Huang L. Modelling and control of two robotic manipulators handling a constrained object. Appl Math Model. 2000;24(12):881–898. doi: 10.1016/S0307-904X(00)00022-6
[29] Kokotovic P, Khalil HK, O'Reilly J. Singular perturbation methods in control: analysis and design. Philadelphia: SIAM; 1999.
[30] Huang A-C, Chien M-C. Adaptive control of robot manipulators: a unified regressor-free approach. Hy: World Scientific Publishing Company; 2010.
[31] Zheng-Hua L, Guo B. Further theoretical results on direct strain feedback control of flexible robot arms. IEEE Trans Automat Contr. 2002;40(4):747–751. doi:10.1109/9.376095